Electronic supplementary information (ESI)

A Zincophilic Separator with Directional Alignment and Pore Hydrophilicity towards Stable aqueous Zinc Metal Batteries

Jing Fu[†a], *Dongyang Huang*[†a], *Ying Mei*[b], *and Qiao Ni*[a,c]*

a. Faculty of Arts and Sciences, Beijing Normal University, Zhuhai 519087, P.R. China

b. Research and Development Center for Watershed Environmental Eco-Engineering, Advanced Institute of Natural Sciences, Beijing Normal University, Zhuhai, 519087, PR China

c. Center for Advanced Materials Research, Advanced Institute of Natural Sciences, Beijing Normal University, Zhuhai 519087, China

† These authors contributed equally to this work.

*Corresponding author: niq@bnu.edu.cn (Q. N.)

Author contributions:

Qiao Ni: Providing original idea, supervision, funding acquisition and revising the manuscript. Jing Fu and Dongyang Huang: conducting experiments, data processing and revising the manuscript. Ying Mei: Providing the electrospinning machine and participate in experimental design.

Note S1. Experimental Section

Materials.

Commercial Zn foils (with a purity of 99.99%, thickness 200 um) and Cu foils (purity 99.99%, thincness 9 um) were acquired from Guangdong Canrd New Energy Technology Co.,Ltd.. Prior to utilization, the zinc foils were polished by a scalpel blade. Polyacrylonitrile (average Mw 149000~151000), N, N-Dimethylformamide (>99.9% (GC)), $ZnSO_4 \cdot 7H_2O$ (>99.5%), Zinc trifluoromethanesulfonate ($Zn(OTF)_2$, >98%) were purchased from Aladdin. Vanadium(V) oxide (V_2O_5, >99.6% min) and sodium chloride (NaCl, 99.8%) were ordered from Alfa Aesar.

PZO separator preparation

Configuration of spinning solution: Firstly, 1.941 g PAN powder was weighed and completely dissolved in 12.1 g of DMF solvent. After PAN was completely dissolved, 0.134 g of $Zn(OTF)_2$ salt was slowly added. A transparent spinning solution of PAN@$Zn(OTF)_2$ with a weight percentage of 16% was obtained after magnetic stirring at 25 ℃ for 2 hours.

Spinning parameter setting: Inject the PAN@$Zn(OTF)_2$ spinning solution into the syringe, ensuring it is thoroughly mixed. Choose a 21-gauge needle as the electrospinning needle. The spinning voltage is adjusted to 20 kV, the distance between the spinning needle and the receiver is 18 cm, the spinning environment temperature is maintained 25 ℃, and the humidity is controlled to be lower than 30% rh. The injection speed of spinning solution is controlled at 0.1 ml h^{-1}; The PAN@$Zn(OTF)_2$ nanofibers are deposited continuously along the metal cylinder, then the as-spun PAN@$Zn(OTF)_2$ films can be finally collected from the aluminum collector receiver. The thickness of the separator can be controlled by the amount of spinning fluid added and the spinning time. The PAN separators were obtained as the same processes of the PZO except without adding $Zn(OTF)_2$ salt during spinning solution preparation.

Synthsis of the $NaV_3O_8 \cdot_{1.5}H_2O$ (NVO) cathode

A total of 2 g commercialized V_2O_5 powder was added into 30 ml NaCl solution (2 M)

followed by magnetic stirring for a duration of 96 h under room temperature. The as prepared dark red powders were collected by washed with deionized water and ethanol three times, respectively. They were then dried in a vacuum oven at 70 °C for 15 hours.

Characterization

The X-ray diffractometer (XRD) patterns were obtained by an XRD diffractometer (D8 Advance, Bruker) with Cu kα as the radiation source (λ = 1.5418Å). Scanning electron microscope (SEM) images were obtained from a field emission scanning electron microscope (FESEM, Hitachi/Regulus 8100). Fourier-transformed infrared spectra (FT-IR) were collected on an IR spectrometer (Thermo Scientific Nicolet iS5). Raman spectra were achieved at the LabSpec6 Spectroscopy Suite (HORIBA, FM/ LabSpec6.fm). The contact angels were measured on the contact angle measuring instrument (DSA25S). The Differential scanning calorimetry (DSC) of the separators were detected on the thermal analyzer (STA8000). The mechanical characteristics of various separators were evaluated by the electronic universal testing equipment (CMT6103/ZWICK/Instron 5969).

The electrolyte immersion method was used to determine the electrolyte absorption of the various separators. The separators with the same diameter (12 mm) was first weighed, marked as m_0. and then soaked the separators in 2 M $ZnSO_4$ electrolyte for 2 h. After removing the excess zinc sulfate solution on the surface of the separator with filter paper, the total weight is labelled as m_1 or m_2. The absorption rate of the separator to the electrolyte is calculated by Equation 1.

$$n = \frac{m1 - m0}{m0} \times 100\%$$

Electrochemical measurements

All the electrochemical performances such as Zn-Zn, Zn-Cu, full cell performances were evaluated in the CR2032-type coin cells by using the LAND CT-2001A battery tester. The CV, GCD, EIS, and potentiostatic polarization test measurements were conducted on CHI 660E electrochemical workstation. The cathode was prepared by

mixing NVO, SP and polyvinylidene fluoride (PVDF) with a mass ratio of 7:2:1, with the NMP serving as solvent. The slurry was thereafter spread on carbon paper one by one and then dried in the vacuum oven at 70 °C for 12 h. The mass loading of the NVO cathode materials is ~0.9-1.2 mg cm^{-2}. 2 mol kg^{-1} $ZnSO_4$ is use as the electrolyte. The separators of GF/D, PAN and PZO were punched into small discs with a diameter of 12 mm before use. The activation energy (*Ea*) of the desolvation process combined with different separators were evaluated by the Arrhenius equation using symmetric Zn||Zn cells. Tafel tests were conducted in Zn-Zn cells with various separators using a scanning rate of 1 mV s^{-1} at potential range from −0.2 to 0.2 V. The Zn ion transference numbers of the different separators were obtained by the Bruce-Vincent method according to the following equation:

$$t_{Zn^{2+}} = \frac{I_s(\Delta V - I_0 R_0)}{I_0(\Delta V - I_s R_s)}$$

where ΔV (10 mV) is the applied potential, I_o and I_s are the initial current and steady-state current, respectively. R_o and R_s are the initial resistance and steady-state resistance, respectively.

The diffusion barrier of zinc ions was evaluated by calculating the activation energy (*Ea*) for Zn^{2+} desolvation according to the Arrhenius formula:[1, 2]

$$R_{ct}{}^{-1} = Ae^{\frac{-Ea}{RT}}$$

The R_{ct} denotes the charge transfer resistance, *A* is the frequency factor, *R* stands for the gas constant, and *T* indicates the absolute temperature.

Density Functional Theory (DFT) Computations

All calculations are performed on the CASTEP package, using the Perdew-Burke-Ernzerhof (PBE) to perform all density functional theory (DFT) calculations in generalized gradient approximation (GGA). The cut-off energy is set to 450 eV, and the self-consistent field convergence threshold is 2×10^{-5} eV. A geometry optimization is considered convergent when the force change is smaller than 0.05 eV/Å. the

dispersion interaction is described using Grimme's DFT-D3 method. The Brillouin zone integral is sampled at 1×1×1 monkhorst pack K point.

The finite element modeling (FEM)

The simulation used the physical field interface of the thrice current distribution in the electrochemical module of COMSOL Multiphysics 6.0 software for simulation purposes. The constructed model consists of three domains, from top to bottom, namely electrolyte, separator, and electrolyte near the electrode surface. The dimensions are depicted in the Fig. S1. The physical field employs the thrice current distribution, deformation geometry, and multiple physical fields reference undeformed boundaries and deformed electrode surfaces. The cubic current distribution module is capable of resolving several parameters such as current, ion concentration distribution, chemical reaction rate, ion electric field migration. It is well-suited for this particular scenario.

The conditions of electrolyte domain are as follows: (1) Diffusion coefficient D_Zn of zinc ions in electrolyte; (2) Electric field migration of zinc ion; (3) Initial conductivity sigma, and conductivity changes with ion concentration; (4) Initial zinc particle concentration Cinit (set at the top boundary); (5) Total electrolyte current density is set at 1000 A/m^2 (top boundary). The conditions of the separator domain are are set according to diffusion coefficients of Zn^{2+} in various separators, the initial conductivity sigma, the conductivity changes with the ion concentration, the electrolyte volume fraction was used to characterize the porosity of the diaphragm and the electric field migration of zinc ion.

The conditions for setting the electrolyte domain near the electrode surface are as follows: (1) Density of deposited zinc is 7140 (kg/m^3), molar mass is 0.065 (kg/mol); (2) Stoichiometric coefficient; (3) Electric field migration of zinc ions; (4) The diffusion coefficient of zinc ions in this area; (5) Electrode surface deposition deformation. The research is set up in two steps: (1) The current distribution is initialized, and the initial electric field is calculated steady-state to improve the convergence of subsequent transient calculations; (2) Transient state. time range (0, 1 s, and 10 s).

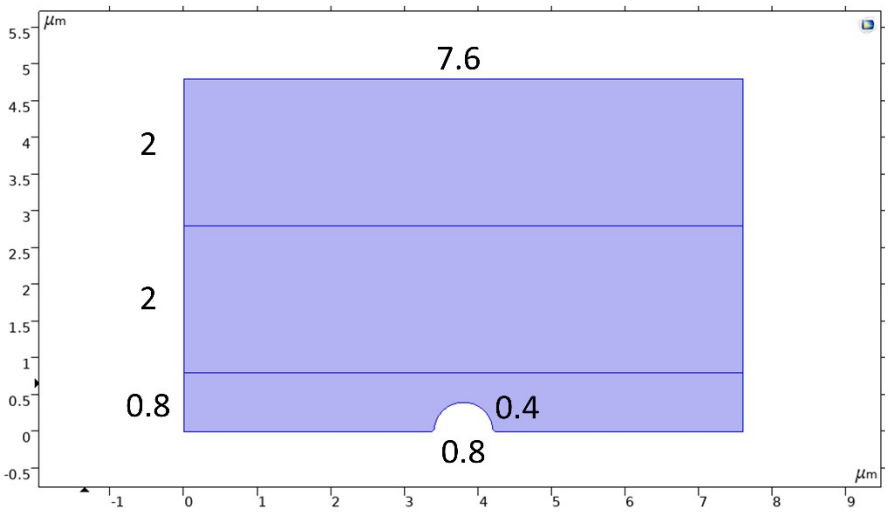

Fig. S1 the simulation model domains and dimensions in this work

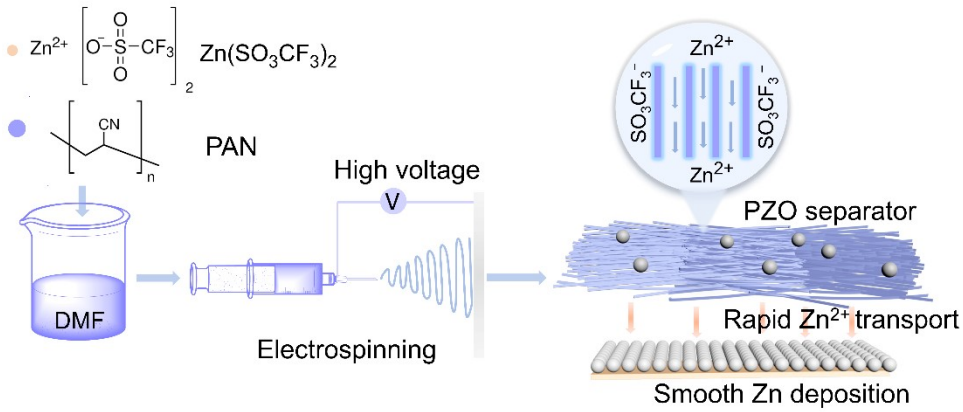

Fig. S2 Schematic illustration of the preparation of PZO separator and Zn deposition behaviors with the PZO separator.

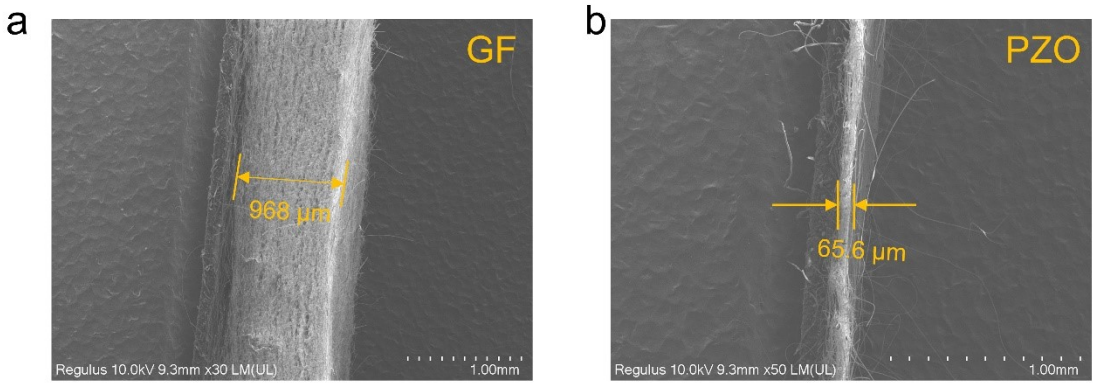

Fig. S3 Cross sectional view of the (a) commercialized GF/D separator; (b) PZO separator

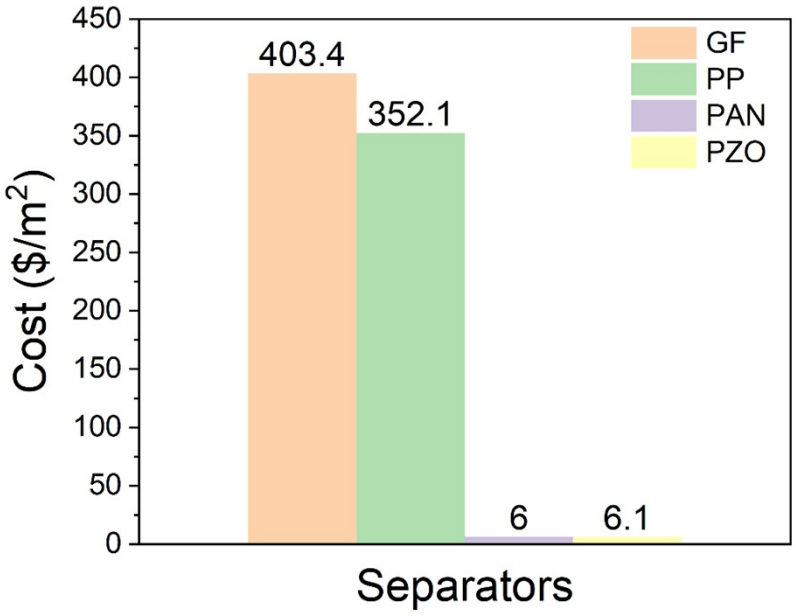

Fig S4. The cost of different separators per square meter (the price of GF/D separator and PP separator were collected from the website of Guangdong Canrd New Energy Technology Co., Ltd).

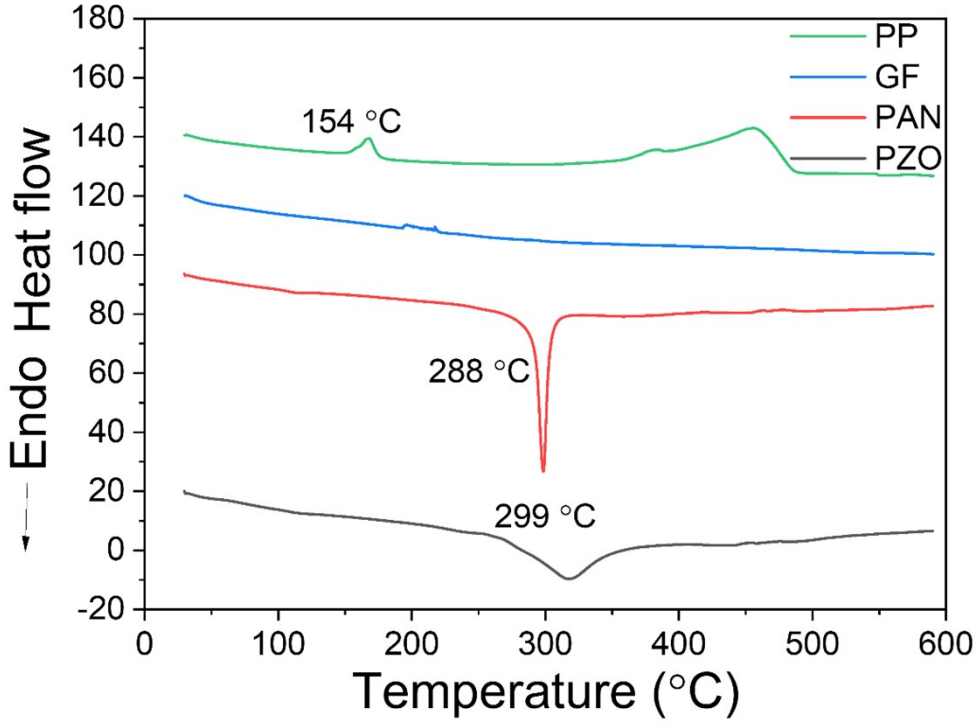

Fig. S5. DSC analysis of the PZO separator and comparison of the thermal stability test of the GF, PAN and PP separators.

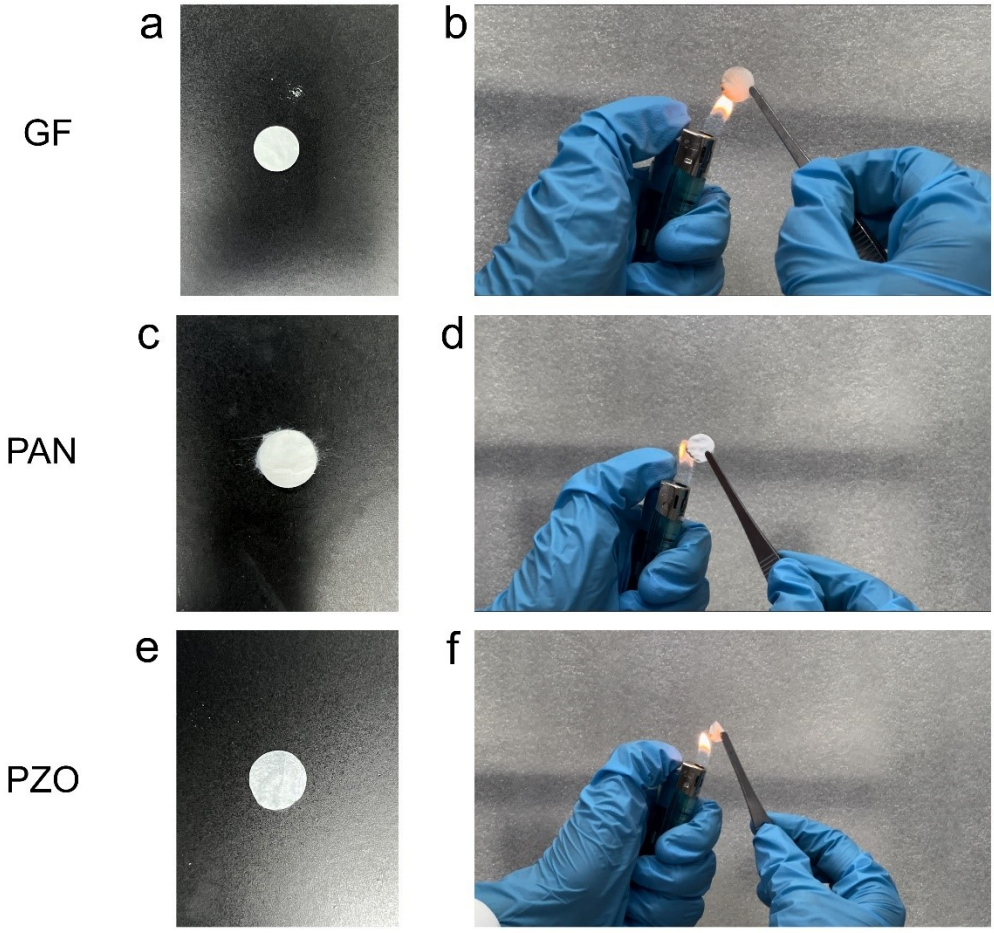

Fig. S6 Thermal stability and flammability of each separator at elevated temperature after 5s: GF (a, b), PAN (c, d), PZO (e, f).

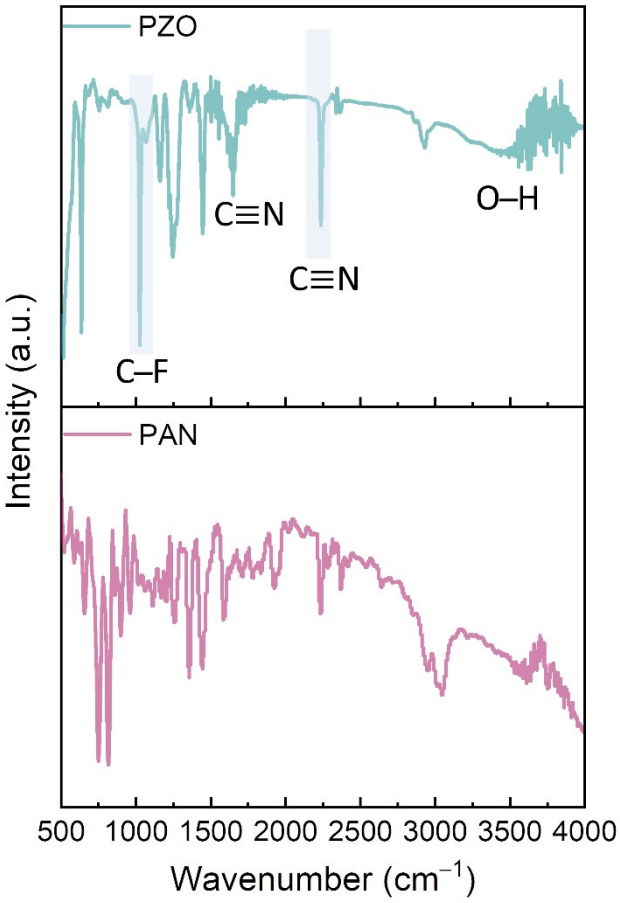

Fig. S7. FTIR spectra of PZO and PAN separators.

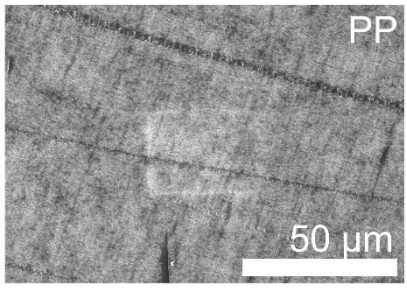

Fig. S8 SEM images of the top view of the PP separator.

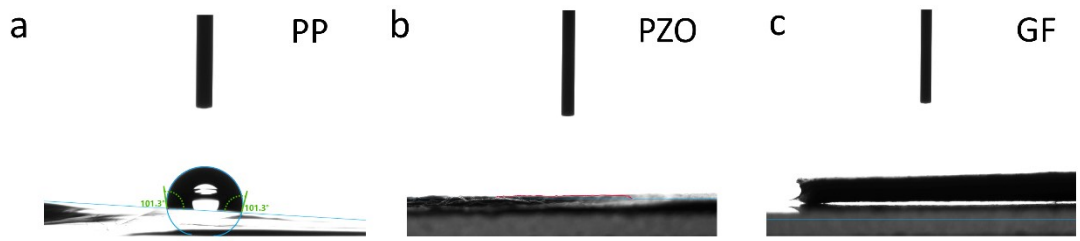

Fig. S9 Contact angels test of the different separators: (a) PP; (b) PZO; (c) GF separators.

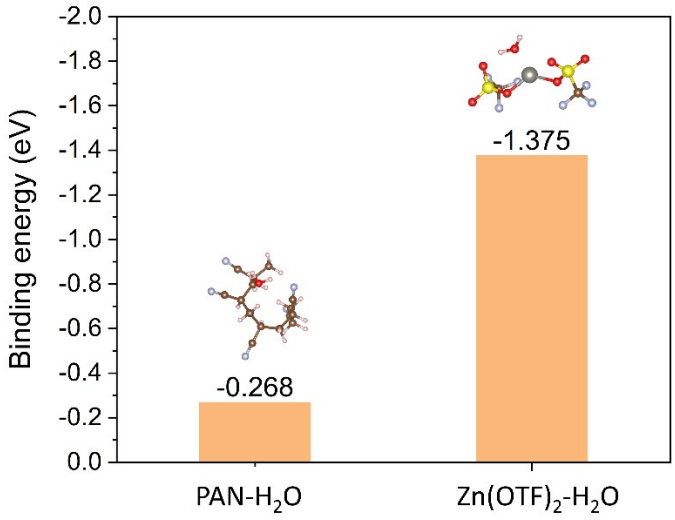

Fig. S10 Calculated binding energy of the PAN-H_2O and $Zn(OTF)_2$-H_2O.

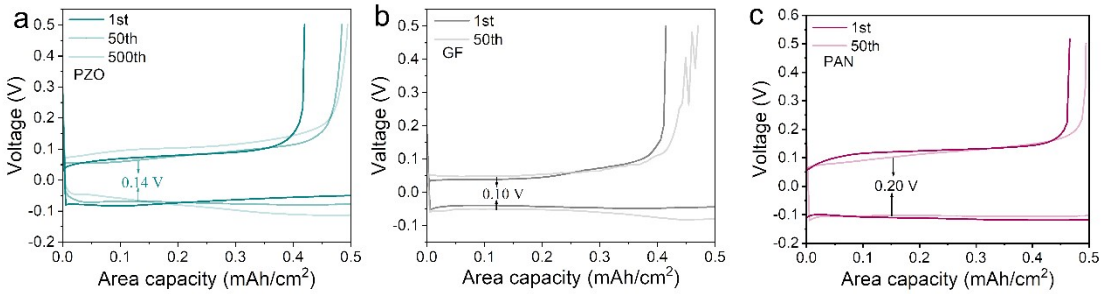

Fig. S11 The Zn-Cu GCD profiles of the cell collected from Fig. 2a coupled with difference separators: (a)PZO; (b) GF; (c) PAN.

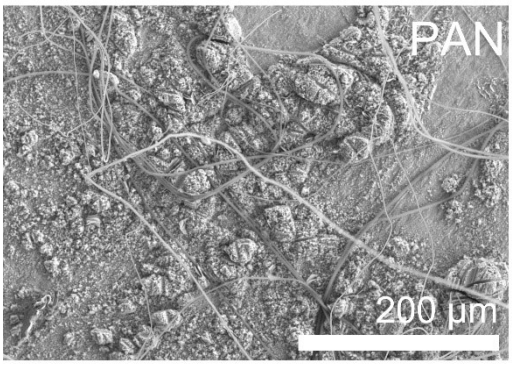

Fig. S12 SEM image of the top view of the zinc deposits on the Cu foil after the first plating process with PAN separator.

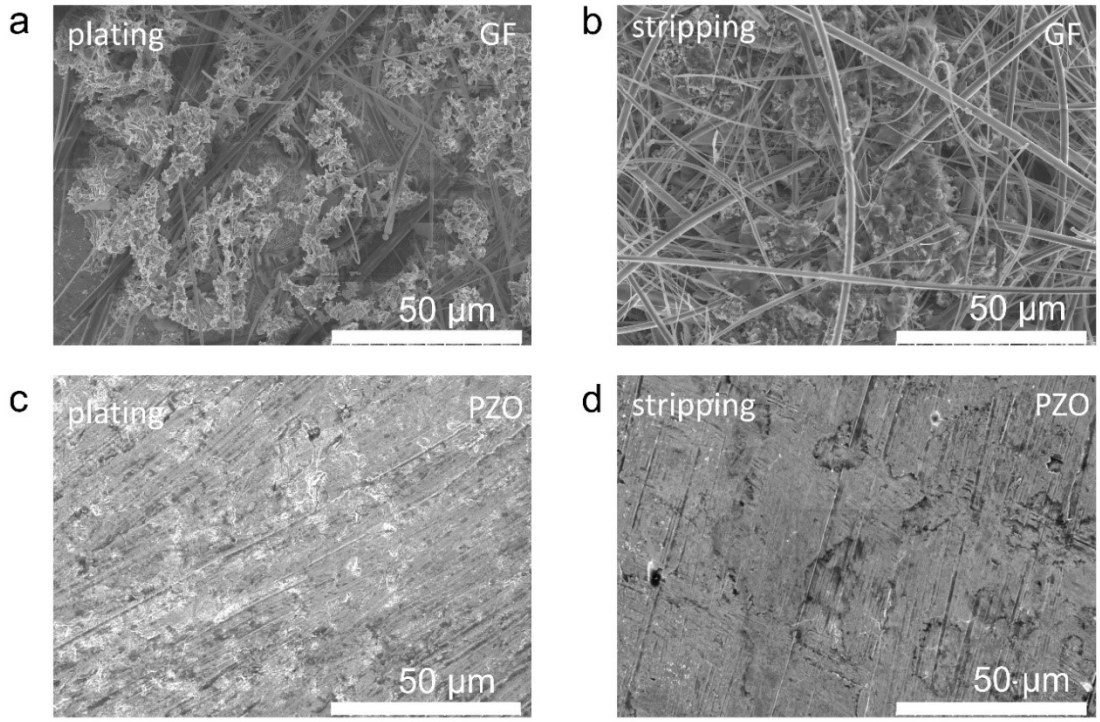

Fig. S13 Comparison of morphologies of plated and stripped Zn with the GF and PZO separators after fifth cycles in symmetrical Zn-Zn cells. A fixed current density of 1 mA cm^{-2} was applied.

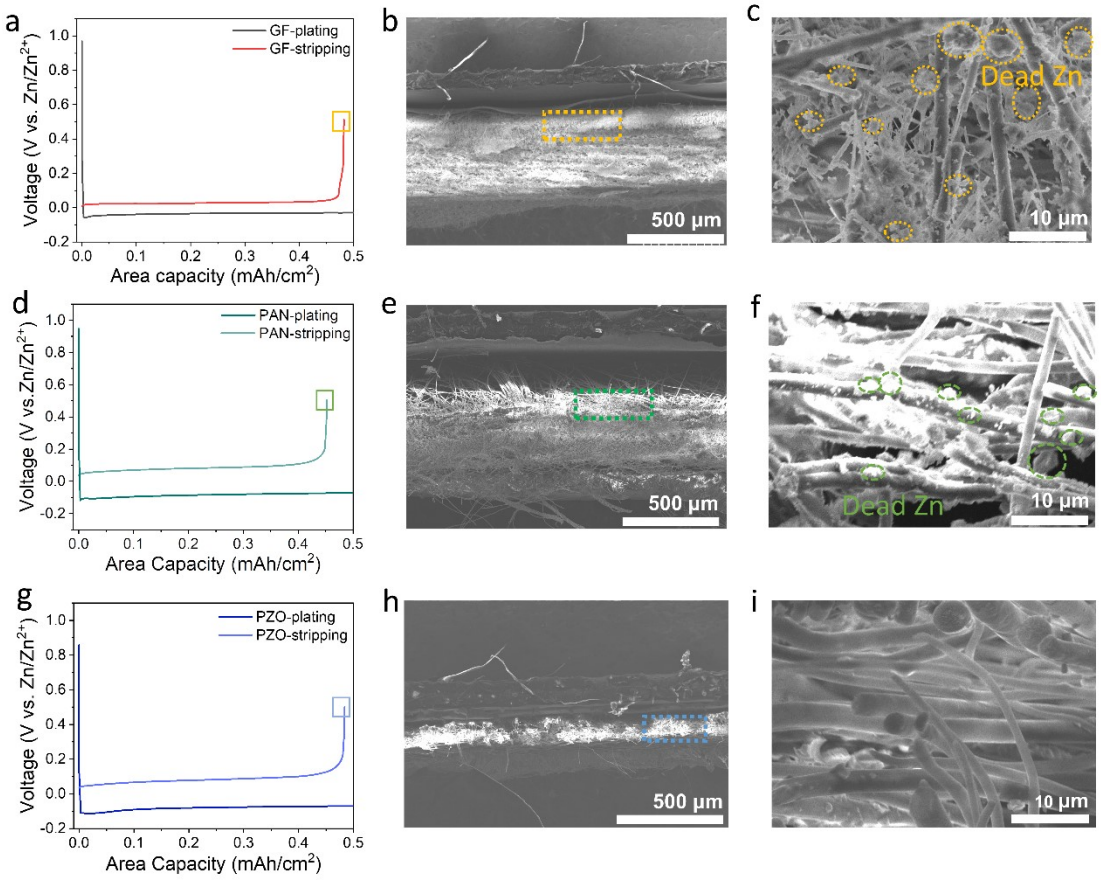

Fig. S14 Cross-sectional morphology of plated zinc on separator/Cu foil double layers at a current density of 1 mA cm^{-2}. The default area capacity is 0.5 mAh cm^{-2}. Voltage and current profiles of zinc plating/stripping on Cu foil with (a) GF, (d) PAN and (g) PZO separators. Cross-sectional SEM images for (b) GF, (e) PAN and (h) PZO separators. Their zoomed-in views are depicted in (c, f, i), correspondingly.

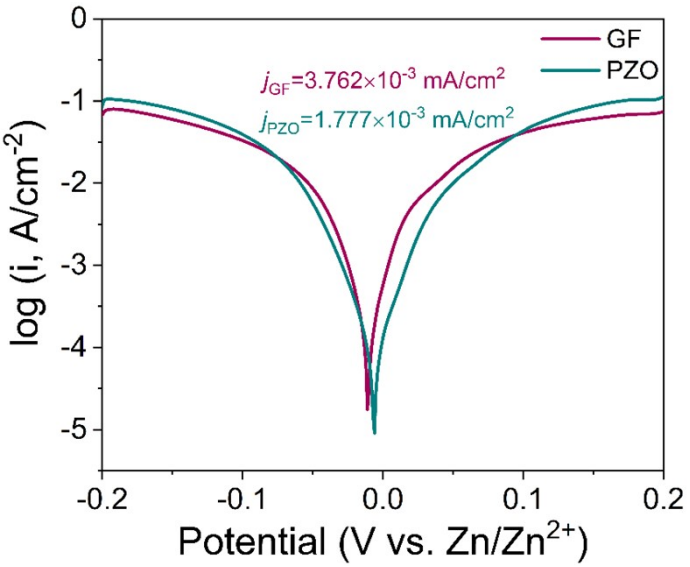

Fig. S15 Tafel curves tests of Zn anodes by various separators in Zn-Zn cells using a scanning rate of 1 mV s^{-1} at potential range from −0.2 to 0.2 V.

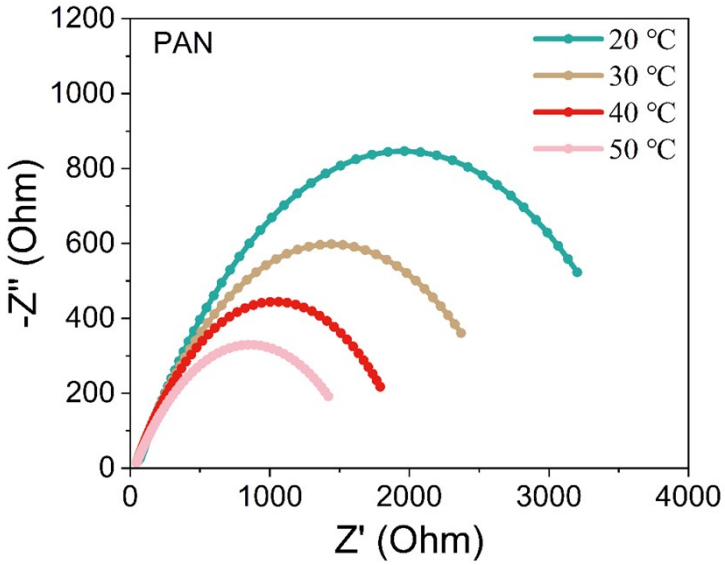

Fig. S16 Nyquist plots for symmetrical Zn-Zn cell using PAN separator at temperatures from 20 to 50 ℃.

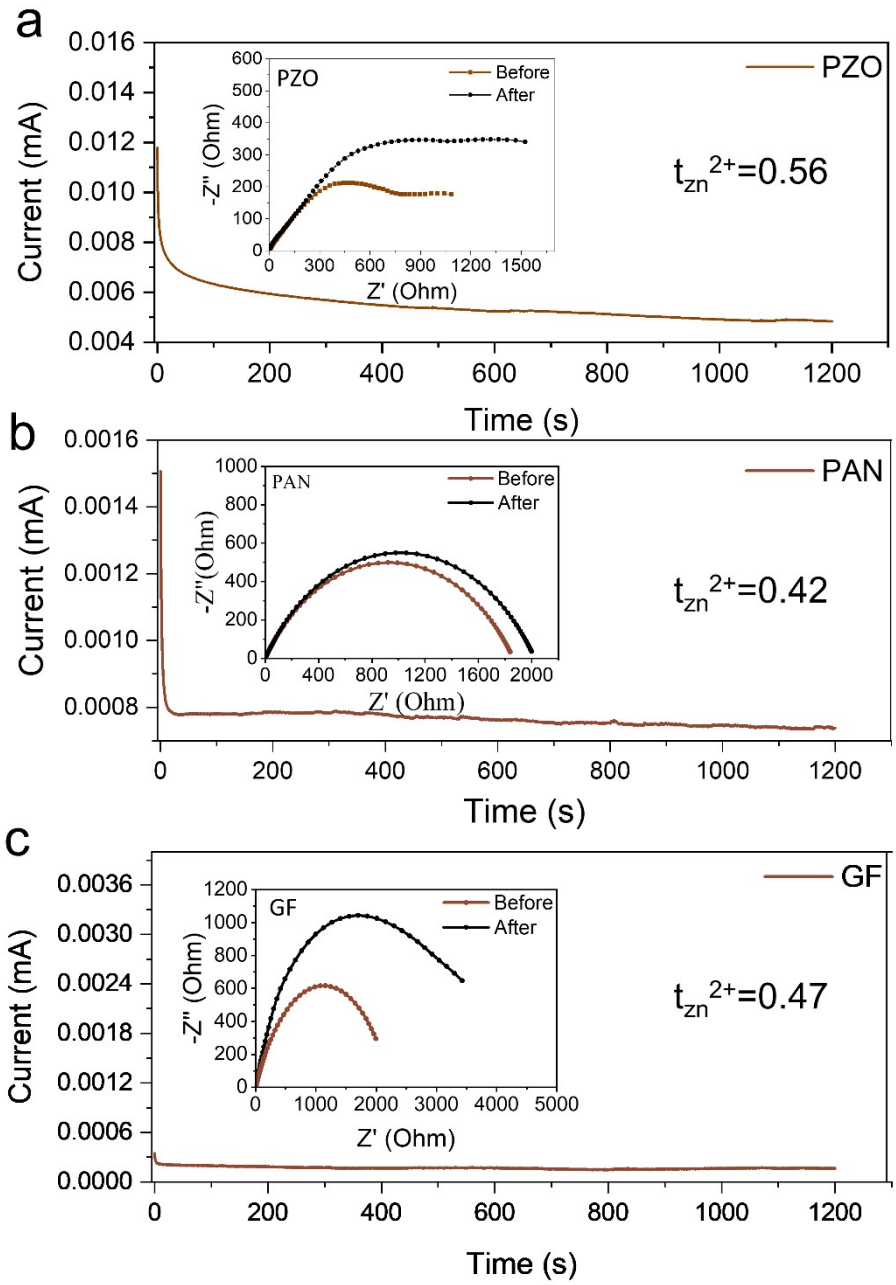

Fig. S17 Current-time plots of Zn||Zn cell with various separators (the inset is the EIS spectra collected before and after polarization process): (a) PZO; (b) PAN; (c) GF.

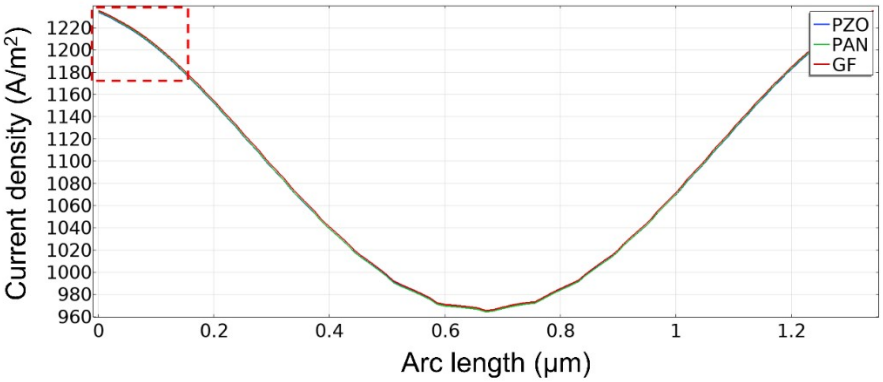

Fig. S18 Relationship between current density and ARC length using various separators.

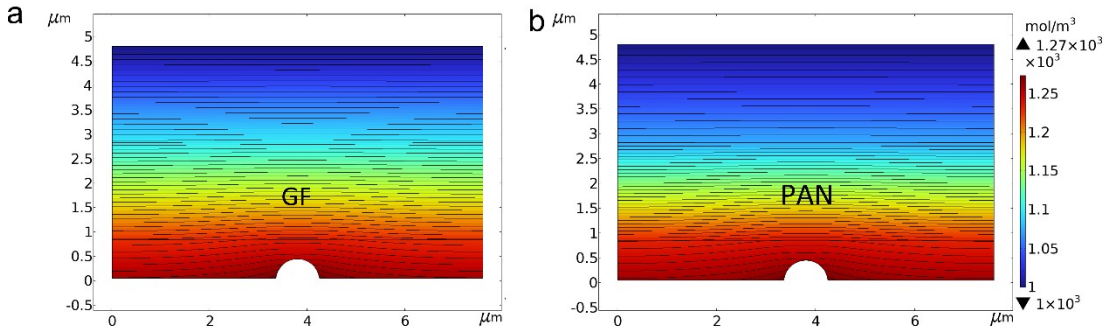

Fig. S19 The models of the zinc ion concentration field models on Zn anode assembled with the (a) GF and (b) PAN separators.

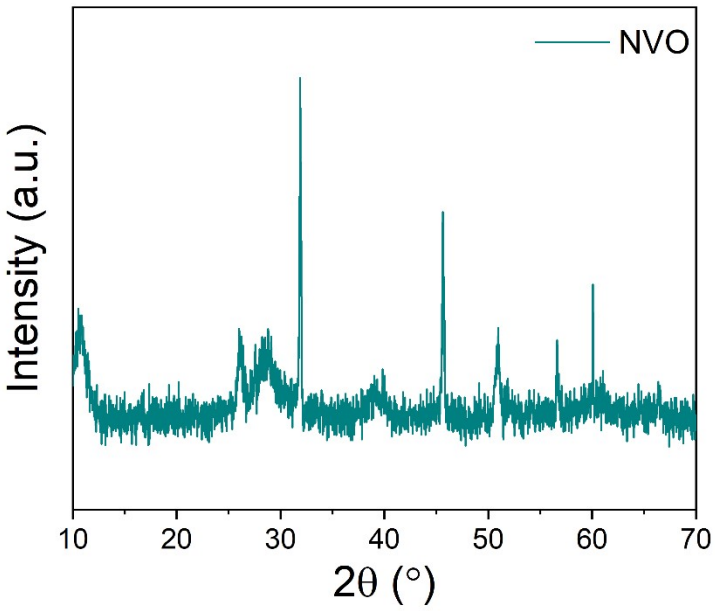

Fig. S20 XRD pattern of the prepared NVP cathode

Table S1. Comparison of basic parameters of different separators.

	PZO	PAN	GF
Thickness (μm)	65.6	140	968
m_o (mg)	0.79	2.91	14.39
m_1 (mg)	21.37	81.48	172.12
m_2 (mg)	20.58	78.57	157.73
Absorbency	26.1%	27%	11.0%
Absorbency per unit thickness	39.8%	19.2%	1.1%

Table S2 Electrochemical performance comparison of the symmetrical Zn-Zn cells with various separators

Separator type	Current density (mA/cm^2)	Time (h)	Ref.
PAN separator	0.283	800	3
TiO_2-PE separator	1	500	4
PBC@cellulose-filter paper	1	322	5
CT@NZF@N separator	0.5	300	6
Nanocellulose membranes	1	100	7
Vertical graphene@glass fibers	1	250	8
water-retaining plant fiber separator	1	300	9
PZO separator	1	900	**This work**

References:

1 C. Meng, W. He, L. Jiang, Y. Huang, J. Zhang, H. Liu and J. J. Wang, *Adv. Funct. Mater.*, 2022, **32**, 2305098.

2 H. Raza, S. Bai, J. Cheng, S. Majumder, H. Zhu, Q. Liu, G. Zheng, X. Li and G. Chen, *Electrochem. Energy Rev.*, 2023, **6**, 14.

3 Y. Fang, X. Xie, B. Zhang, Y. Chai, B. Lu, M. Liu, J. Zhou and S. Liang, *Adv. Funct. Mater.*, 2022, **32**, 2109671.

4 K. Yu, Y. Wen, M. Yan, X. Teng, W. Yang, S. Lian, J. Zhang, F. Zhang, X. Jiang and Y. Luo, *Mater. Today Energy*, 2024, **40**, 101488.

5 L. Li, J. Peng, X. Jia, X. Zhu, B. Meng, K. Yang, D. Chu, N. Yang and J. Yu, *Electrochim Acta*, 2022, **430**, 141129.

6 G. Guo, X. Tan, K. Wang, L. Zheng and H. Zhang, *J Power Sources*, 2023, **553**, 232321.

7 X. Ge, W. Zhang, F. Song, B. Xie, J. Li, J. Wang, X. Wang, J. Zhao and G. Cui, *Adv. Funct. Mater.*, 2022, **32**, 2200429.

8 C. Li, Z. Sun, T. Yang, L. Yu, N. Wei, Z. Tian, J. Cai, J. Lv, Y. Shao and M. H. Rümmeli, *Adv Mater*, 2020, **32**, 2003425.

9 B. Hao, H. Yang, Z. Wang, Z. Xie, C. Zhu, W. Chen, L. Zhang, J. Liu, C. Yan and J. Zhou, *J. Phys. Chem. Lett.*, 2023, **14**, 9986-9995.